

Strained Ruthenium Complexes Are Potent Light-Activated Anticancer Agents

Brock S. Howerton,[‡] David K. Heidary,[‡] and Edith C. Glazer*[‡]

Department of Chemistry, University of Kentucky, Lexington, Kentucky 40506, United States

S Supporting Information

ABSTRACT: Strained ruthenium (Ru) complexes have been synthesized and characterized as novel agents for photodynamic therapy (PDT). The complexes are inert until triggered by visible light, which induces ligand loss and covalent modification of DNA. An increase in cytotoxicity of 2 orders of magnitude is observed with light activation in cancer cells, and the compounds display potencies superior to cisplatin against 3D tumor spheroids. The use of intramolecular strain may be applied as a general paradigm to develop light-activated ruthenium complexes for PDT applications.

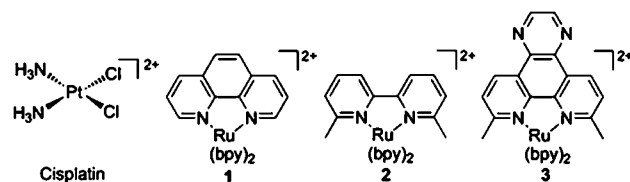
Photoactivation is an elegant method to convert nontoxic prodrugs to active cytotoxic species in a spatially and temporally controlled manner. This provides a mechanism to discriminate between malignant tissues of tumors and the surrounding healthy tissues, potentially reducing the dose-limiting side effects incurred with standard chemotherapies. Photodynamic therapy (PDT) uses this light-targeted approach, and has been successfully applied in the treatment of various cancers, notably of the lung, esophagus, and skin.^{1,2} Commonly, PDT requires a photosensitizer such as a porphyrin to generate singlet oxygen (¹O₂), which is the actual toxic moiety. This requirement for oxygen has limited the utility of PDT, due to the hypoxic nature of many tumors. Improved PDT agents are required, and the challenge is to develop compounds that are thermally inert, but can be triggered by low energy, visible light to generate toxic species as potent as standard chemotherapeutics. Other desired features include ease of synthesis and retention of activity in the presence of biological reducing agents such as glutathione (GSH), which inactivate platinum (Pt) drugs.³ Structural motifs that are distinct from those of square planar platinum compounds would be advantageous, in that they could potentially address cancer types that are resistant to cisplatin and its analogues. This has motivated investigation of multiple metal centers with alternative geometries as potential light-activated therapeutics.⁴ However, a key characteristic that is lacking in the existing metal-based PDT agents is a flexible design strategy that allows for facile modification of chemical structure without loss of activity.

Ru(II) complexes are three-dimensional, in contrast to the square planar Pt(II) compounds, and each of the ligands may be readily changed to modify the structure of the complex. Most importantly, these compounds are particularly attractive for photoactivated biological applications, as they possess

tunable photophysical properties, absorb strongly in the visible region ($\lambda_{\text{max}} \sim 450 \text{ nm}$), and are kinetically inert.⁵ While most Ru(II) polypyridyl complexes are also quite photostable, it is known that complexes with distorted octahedral geometry photodecompose via ligand dissociation. This is a result of population of low-lying ³d-d* states, which can be thermally accessed from the ³MLCT (metal-to-ligand charge transfer) excited state.^{6,7} We have utilized these steric and electronic features to create Ru(II) complexes that are potential PDT agents. The compounds are stable in the dark, but react rapidly upon photoexcitation with visible (>450 nm) light to eject a ligand and cross-link DNA. The compounds maintain good reactivity in the presence of GSH, are nontoxic in the dark, and are cytotoxic upon light activation, providing greater potency than cisplatin.

Three complexes with key structural differences were explored to test the strain-mediated photoactivation approach (Chart 1). The complexes were synthesized and characterized

Chart 1. Structures of Metal Complexes Included in This Study



as a racemic mixture of Δ and Λ enantiomers. Ru(bpy)₂phen (1), a known low affinity DNA binder,⁸ was used as an unstrained control. To distort the geometry about the octahedral metal center, polypyridyl ligands with methyl substituents were incorporated into the Ru(II) complexes; these groups are directed toward the other coordinating ligands, causing steric clashes. The complexes were readily prepared under low light conditions by refluxing the precursor Ru(bpy)₂Cl₂ with the desired ligand in ethylene glycol. They were purified by silica gel flash chromatography, and converted to chloride salts for testing.

Addition of the methyl groups to either bpy (2,2'-bipyridyl) or the DNA intercalating ligand dpq (dipyrido[3,2-*f*:2',3'-*h*]-quinoxaline)⁹ results in complexes that undergo photochemical reactions upon exposure to light. Irradiation of 2 and 3 in either acetonitrile or buffer with >450 nm light using a 200 W

Received: January 30, 2012

Published: May 3, 2012

projector and cutoff filters resulted in substitution of solvent molecules for the polypyridyl ligand. The photochemical reaction was conveniently followed by UV/vis absorption spectroscopy, as shown in Figure 1.

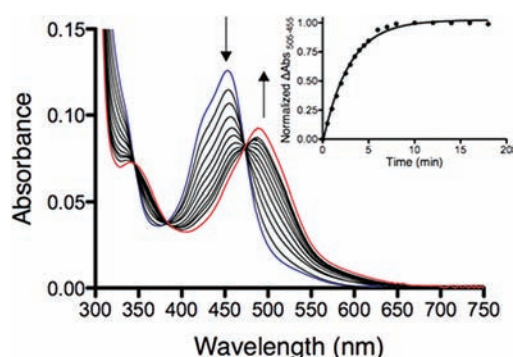


Figure 1. Photoejection of **2** in buffer (10 mM phosphate buffer, pH 7.5) followed by UV/vis absorption. Inset shows the photoejection kinetics, with complete reaction in less than 10 min.

The photoejection is both rapid and selective, with a $t_{1/2}$ of 2 min for **2** and clear isosbestic points at 351, 389, and 476 nm, highlighting the selectivity of the photolabilization. Electrospray ionization mass spectrometry (ESI-MS) experiments identified the ejection of the 6,6'-dimethyl-2,2'-bpy ligand from compound **2**, while compound **3** ejects the 2,9-dimethyl-dpq ligand. The reaction goes to completion for **2**, as shown in Figure S13. The reaction kinetics are 30-fold faster for **2** than for **3** (see Figures S2 and S3), likely due to the rigidity of the dpq ligand, which could enhance rechelation, interfering with the stepwise dissociative bond breaking mechanism that releases the ligand.^{6b,10–12} In contrast to both **2** and **3**, the control compound **1** is photostable under the irradiation conditions used. Finally, in the dark, all complexes are stable in aqueous solution at concentrations of 50 μ M for months at room temperature.

DNA damage was analyzed by gel electrophoresis, as shown in Figure 2. Cisplatin kinks DNA and causes unwinding, reducing its mobility on agarose gels¹³ and impeding

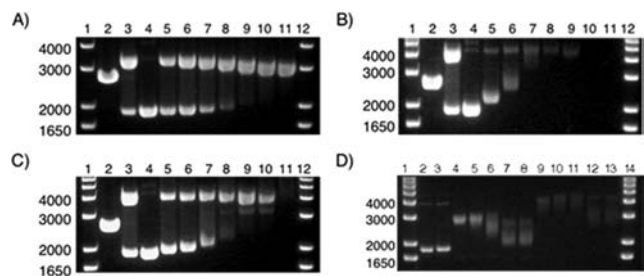


Figure 2. Agarose gel electrophoresis of 40 μ g/mL pUC19 plasmid (10 mM phosphate buffer, pH 7.5) with light-activated Ru(II) compounds and cisplatin. The supercoiled plasmid form migrates at 2000 bp, relaxed circle form is \sim 4000 bp, and linear form is just below 3000 bp. Dose response profiles: (A) **1**; (B) **2**; (C) **3**. Lanes 1 and 12, DNA molecular weight standard; lane 2, linear pUC19; lane 3, relaxed circle ($\text{Cu}(\text{phen})_2$ reaction with pUC19); lanes 4–11, 0, 7.5, 15, 30, 60, 120, 240, and 500 μ M compound. (D) Effect of GSH on DNA cross-linking. Lanes 1 and 14, DNA molecular weight standard; lane 2, pUC19; lane 3, pUC19 + 40 mM GSH. Cisplatin (30 μ M, lanes 4–8) and compound **2** (30 μ M, lanes 9–13) were dosed with GSH: lanes 4–8 and 9–13, 0.01, 0.1, 1, 10, 40 mM GSH.

intercalation of ethidium bromide (EtBr).¹⁴ $\text{Cu}(\text{phen})_2$ produces single strand breaks, generating relaxed circular plasmid DNA.¹⁵ Exposure of ruthenium compounds **1–3** to visible light (200 W, 1 h) in the presence of pUC19 plasmid produces both these distinct effects: DNA photocleavage (in the case of compound **1**), and DNA photobinding, which may be cross-linking (in the case of **2**). Compound **3** exhibits a combination of these two mechanisms. Light-induced DNA single strand breaks produced by **1** are clear from the conversion of supercoiled DNA to relaxed circular form (Figure 2A). DNA photobinding is clear for **2** and **3**, as the supercoiled DNA migrates more slowly through the gel and EtBr intercalation is diminished with increasing concentration of the Ru(II) complexes (Figure 2B,C). An additional form is observed with high concentrations of **3** that migrates more quickly than the relaxed circular form (see Figure 2C, lanes 8–10). In the absence of light, no DNA damage or binding is observed, as shown in Figure S6.

Nucleophilic sulfur-containing molecules such as GSH are key agents in the detoxification of cisplatin, and are present in millimolar concentrations in cells.³ Cisplatin binds to GSH rapidly, inactivating the drug and inhibiting reaction with DNA. In contrast, prodrug compounds **2** and **3** show no interaction with GSH over a period of days, as observed by UV/vis spectroscopy (see Figure S4). In addition, the photoactivated DNA cross-linking Ru(bpy)₂ species retains its ability to damage DNA, even at high GSH concentrations. Figure 2D shows the cross-linking of plasmid DNA by cisplatin and light-activated compound **2** in the presence of increasing amounts of GSH. Cisplatin exhibits significantly reduced cross-linking efficacy with increasing levels of GSH, as indicated by greater mobility of the DNA on the agarose gel. In contrast, the active form of **2** causes greater DNA binding than cisplatin. These results are consistent with the expectation that the “softer” acid Pt(II) metal complex is more reactive with “soft” nucleophilic thiols and suggests that the Ru(II) complexes will not be significantly detoxified by cellular sulfur compounds. These results are supported by cell viability experiments where cisplatin or compound **2** were co-dosed with increasing concentrations of GSH (see Figure S19). GSH reduces cytotoxicity for cisplatin, but not for **2**.

To determine the potency of the Ru(II) complexes, cell cytotoxicity studies were performed in HL60 leukemia cells and A549 lung cancer cells (see Figure 3 and Table 1). Cells were incubated with compounds for 12 h in the dark before irradiation with >450 nm light (410 W) for 3 min. Dark controls were run in parallel. Cell survival was quantified 72 h later through the use of an ATP luciferase assay, and confirmed by Trypan Blue staining and manual counting. As expected, cisplatin exhibited the same activity under light and dark conditions. Control compound **1**, which causes single strand DNA breaks, exhibited only slightly enhanced activity upon irradiation. In contrast, photoreactive compounds **2** and **3** showed significant light-triggered toxicity. After irradiation, both compounds **2** and **3** produced single μ M IC₅₀ values, as shown in Table 1. The complexes are more potent than cisplatin when light activated, but are nontoxic in the dark, with dark IC₅₀ values over 100 μ M for **3** and no dark toxicity observed up to a concentration of 300 μ M for **2**.¹⁶

The 100–200-fold difference in light and dark IC₅₀ values provides a large potential therapeutic window to allow for selective targeting of cells by exposure to light. To the best of our knowledge, this is the largest phototoxicity index reported

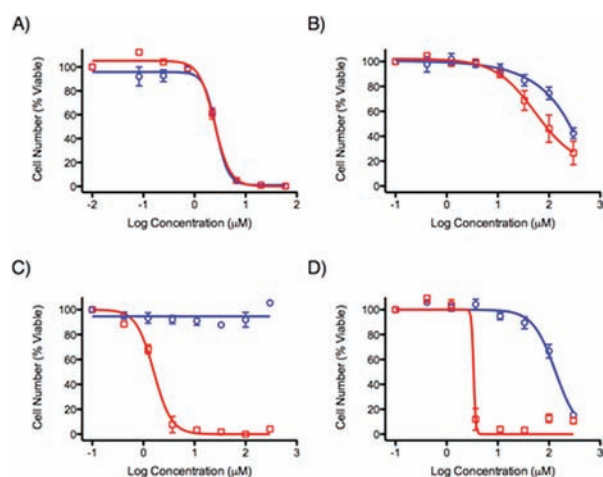


Figure 3. Cytotoxicity dose responses of metal complexes in HL60 cells: (A) cisplatin; (B) 1; (C) 2; (D) 3. Dark conditions (circles, blue line); irradiated samples, 3 min >450 nm light (squares, red line). ($n = 3$).

for a metal complex activated by visible light. In addition, the light activated Ru(II) complexes cause essentially complete cell death, which is often a challenge with light activated cytotoxic systems.

While most initial drug screening is performed in two-dimensional cell culture, it is known that monolayers do not effectively model the characteristics of three-dimensional solid tumors *in vivo*.¹⁷ In contrast, 3D tumor spheroids provide a system that approximates the complexity of *in vivo* tumors.¹⁸

These spheroids mimic the pathophysiology of tumors, including hypoxic/necrotic regions, changes in cell shape, high proportions of quiescent cells, alterations in gene expression profiles, and diminished permeability to drugs. As a result, spheroids exhibit the phenomena of multicellular resistance (MCR), which is manifest in the diminished efficacy of chemotherapeutics to levels similar to *in vivo* activities.^{18d} Thus, to characterize the light-activated ruthenium compounds under more challenging and biologically relevant conditions, efficacy was assessed in a 3D tumor model by forming tumor spheroids with A549 cells.

Spheroids of ca. 600 μm in diameter were dosed with compounds and then either kept in the dark or irradiated with >450 nm light for 3 min (Figure 4). Significant light-selective cytotoxicity was observed for 2, with an IC_{50} value of 21 μM , while no cell death was observed up to 300 μM in the absence of light. Under the same conditions, the IC_{50} for cisplatin fell to 42 μM in the spheroid model, and the PDT drug ALA (aminolevulinic acid) had no effect. The activity of 3 was more

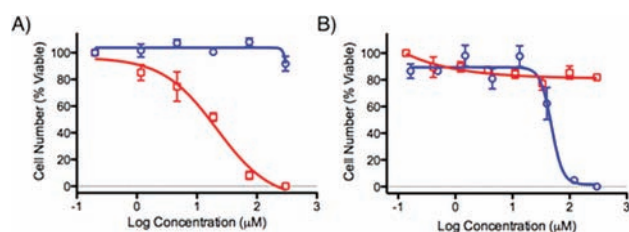


Figure 4. Cytotoxicity dose responses in A549 tumor spheroids. (A) Compound 2: dark conditions (circles, blue line); irradiated samples, 3 min >450 nm light (squares, red line). (B) Cisplatin, dark conditions (circles, blue line). ALA, irradiated samples, 3 min >450 nm light (squares, red line). ($n = 3$).

diminished than 2 in the spheroid, with a light-activated IC_{50} of 64 μM . It is likely that a greater light dose is required for full activation of 3 in the 3D model than is provided in the 3 min of irradiation.

This retention in potency for 2 in 3D tissue culture is promising, and the compounds exhibited twice the potency of cisplatin in both monolayer and tumor spheroids. The MCR index value is low for 2, similar to cisplatin (see Table 1). This is especially noteworthy, considering that the MCR value for cisplatin is much lower than for many other chemotherapeutics.¹⁹

In conclusion, we have synthesized strained Ru(II) polypyridyl complexes that utilize the steric clash of their ligands to promote visible light mediated ligand expulsion. While unreactive in the dark, these compounds are transformed upon light activation into potent cytotoxic species. As potential PDT agents, these compounds offer key advantages, including ease of synthesis, high solubility, low dark toxicities, and resistance to inactivation by thiol reagents. The DNA damaging mechanism appears to mimic the activity of cisplatin, which would make them potentially amenable to a variety of cancer types, and studies in 3D tumor spheroids demonstrate greater potency than cisplatin. It is anticipated that intramolecular strain may be used as a general mechanism that can be applied to the development of a family of light activated compounds to act as targeted chemotherapeutics. We are currently combining this design strategy with a modular coordination chemistry approach to develop new systems with optimized photophysical and biological properties.

■ ASSOCIATED CONTENT

📄 Supporting Information

Additional synthetic details for 2 and 3, experimental procedures for the photochemical and biological studies, spectra for photoejection experiments and IC_{50} plots. This

Table 1. Cytotoxicity IC_{50} Values in 2D and 3D Cellular Assays^a

compound	light IC_{50} [μM]			dark IC_{50} [μM]			phototoxicity index, PI^b		MCR index ^c
	HL60	A549	A549 spheroid	HL60	A549	A549 spheroid	HL60	A549	
Cisplatin	3.1 (± 0.2)	3.4 (± 0.6)	n.d. ^d	3.1 (± 0.1)	3.5 (± 0.6)	42 (± 3.6)	1	1	12.4
1	81 (± 1.9)	40 (± 4)	>300	240 (± 9)	250 (± 5)	>300	3	6.3	>7.5
2	1.6 (± 0.2)	1.1 (± 0.3)	21.3 (± 2.3)	>300	150 (± 7)	>300	>188	136	19.4
3	2.6 (± 1.0)	1.2 (± 0.1)	64.6 (± 4.7)	108 (± 1.9)	250 (± 5)	>300	42	208	54
ALA	16.2 (± 3.2)	21 (± 3.5)	>300	>300	87.8 (± 5.5)	>300	>18	4.2	>14

^a IC_{50} values are averages from three measurements. ^bThe phototoxicity index (PI) is the ratio of the dark and light IC_{50} values. ^cThe multicellular resistance (MCR) index is the ratio of the spheroid and monolayer culture IC_{50} values. ^dn.d.= not determined; see dark IC_{50} value.

material is available free of charge via the Internet at <http://pubs.acs.org>.

AUTHOR INFORMATION

Corresponding Author

ec.glazer@uky.edu

Author Contributions

[‡]These authors contributed equally.

Notes

The authors declare no competing financial interest.

ACKNOWLEDGMENTS

We thank the Elsa U. Pardee Foundation and the American Cancer Society (IRG-85-001-22) for their generous support of this work. E.C.G. thanks Prof. Damien Jouvenot for helpful discussions and Prof. Mark Lovell for use of tissue culture facilities. Additional chemical and biological analysis was performed at the University of Kentucky Environmental Research Training Laboratory (ERTL).

REFERENCES

- (1) Vrouenraets, M. B.; Visser, G. W.; Snow, G. B.; van Dongen, G. A. *Anticancer Res.* **2003**, *23* (1B), 505–522.
- (2) Dolmans, D. E.; Fukumura, D.; Jain, R. K. *Nat. Rev. Cancer* **2003**, *3* (5), 380–387.
- (3) Cepeda, V.; Fuertes, M. A.; Castilla, J.; Alonso, C.; Quevedo, C.; Perez, J. M. *Anticancer Agents Med. Chem.* **2007**, *7* (1), 3–18.
- (4) For illustrative octahedral platinum complexes see (a) Farrer, N. J.; Woods, J. A.; Salassa, L.; Zhao, Y.; Robinson, K. S.; Clarkson, G.; Mackay, F. S.; Sadler, P. J. *Angew. Chem., Int. Ed.* **2010**, *49* (47), 8905–8908. (b) Mackay, F. S.; Woods, J. A.; Heringova, P.; Kasparkova, J.; Pizarro, A. M.; Moggach, S. A.; Parsons, S.; Brabec, V.; Sadler, P. J. *Proc. Nat. Acad. Sci. U.S.A.* **2007**, *104* (52), 20743–20748. Ruthenium complexes: (c) Singh, T. N.; Turro, C. *Inorg. Chem.* **2004**, *43* (23), 7260–7262. (d) Monro, S.; Scott, J.; Chouai, A.; Lincoln, R.; Zong, R.; Thummel, R. P.; McFarland, S. A. *Inorg. Chem.* **2010**, *49* (6), 2889–2900. Rhodium complexes: (e) Mahnken, R. E.; Billadeau, M. A.; Nikonowicz, E. P.; Morrison, H. *J. Am. Chem. Soc.* **1992**, *114* (24), 9253–9265. (f) Lutterman, D. A.; Fu, P. K. L.; Turro, C. *J. Am. Chem. Soc.* **2006**, *128* (3), 738–739. Mixed metal complexes: (g) Wang, J.; Higgins, S. L. H.; Winkel, B. S. J.; Brewer, K. J. *Chem. Commun.* **2011**, *47* (35), 9786–9788. (h) Higgins, S. L.; Tucker, A. J.; Winkel, B. S.; Brewer, K. J. *Chem. Commun.* **2012**, *48* (1), 67–69.
- (5) Juris, A.; Balzani, V.; Barigelletti, F.; Campagna, S.; Belser, P.; Vonzelewsky, A. *Coord. Chem. Rev.* **1988**, *84*, 85–277.
- (6) (a) Van Houten, J.; Watts, R. J. *J. Am. Chem. Soc.* **1976**, *98* (16), 4853–4858. (b) Durham, B.; Caspar, J. V.; Nagle, J. K.; Meyer, T. J. *J. Am. Chem. Soc.* **1982**, *104* (18), 4803–4810. (c) Ford, P. C. *Coord. Chem. Rev.* **1982**, *44* (1), 61–82. (d) Durham, B.; Walsh, J. L.; Carter, C. L.; Meyer, T. J. *Inorg. Chem.* **1980**, *19* (4), 860–865.
- (7) This has been applied to the creation of molecular devices; see (a) Baranoff, E.; Barigelletti, F.; Bonnet, S.; Collin, J. P.; Flamigni, L.; Mobian, P.; Sauvage, J. P. *Photofunct. Transition Met. Complexes* **2007**, *123*, 41–78. (b) Mobian, P.; Kern, J. M.; Sauvage, J. P. *Angew. Chem., Int. Ed.* **2004**, *43* (18), 2392–2395. (c) Collin, J. P.; Jouvenot, D.; Koizumi, M.; Sauvage, J. P. *Inorg. Chem.* **2005**, *44* (13), 4693–4698.
- (8) Lincoln, P.; Norden, B. *J. Phys. Chem. B* **1998**, *102* (47), 9583–9594.
- (9) (a) Greguric, I.; Aldrich-Wright, J. R.; Collins, J. G. *J. Am. Chem. Soc.* **1997**, *119* (15), 3621–3622. (b) Collins, J. G.; Sleeman, A. D.; Aldrich-Wright, J. R.; Greguric, I.; Hambley, T. W. *Inorg. Chem.* **1998**, *37* (13), 3133–3141. (c) Collins, J. G.; Aldrich-Wright, J. R.; Greguric, I. D.; Pellegrini, P. A. *Inorg. Chem.* **1999**, *38* (24), 5502–5509.
- (10) Tachiyashiki, S.; Ikezawa, H.; Mizumachi, K. *Inorg. Chem.* **1994**, *33* (4), 623–625.
- (11) Laemmel, A. C.; Collin, J. P.; Sauvage, J. P. *Eur. J. Inorg. Chem.* **1999**, *3*, 383–386.
- (12) Compound **3** is susceptible to additional photochemical reactions when subjected to irradiation for long times, as shown in Figures S2 and S3.
- (13) Keck, M. V.; Lippard, S. J. *J. Am. Chem. Soc.* **1992**, *114* (9), 3386–3390.
- (14) Demeunynck, M.; Bailly, C.; Wilson, W. D. *Small Molecule DNA and RNA Binders: From Synthesis to Nucleic Acid Complexes*; Wiley-VCH: New York, 2003.
- (15) Keck, M. V. *J. Chem. Educ.* **2000**, *77* (11), 1471–1473.
- (16) The slightly higher dark toxicity value for **3** is attributed to the higher DNA affinity of the preactivated complex.
- (17) Abbott, A. *Nature* **2003**, *424* (6951), 870–872.
- (18) (a) Friedrich, J.; Seidel, C.; Ebner, R.; Kunz-Schughart, L. A. *Nat. Protoc.* **2009**, *4* (3), 309–324. (b) Kunz-Schughart, L. A.; Freyer, J. P.; Hofstaedter, F.; Ebner, R. *J. Biomol. Screening* **2004**, *9* (4), 273–85. (c) Herrmann, R.; Fayad, W.; Schwarz, S.; Berndtsson, M.; Linder, S. *J. Biomol. Screen* **2008**, *13* (1), 1–8. (d) Desoize, B.; Jardillier, J. *Crit. Rev. Oncol. Hematol.* **2000**, *36* (2–3), 193–207.
- (19) There is commonly a large discontinuity in 2D IC₅₀ and in vivo activity for anticancer agents that is reflected in the MCR value. For example, etoposide has an MCR of 163, and vineblastine has been measured to have an MCR of 6625. As a result, 3D IC₅₀ values are considered more indicative of appropriate dosing parameters in vivo. See ref 18d.